PLI-Signal Quality RWA algorithm for Limited Range Wavelength Converter based Translucent Optical Wavelength Division Multiplexed (WDM) Networks

Sridhar Iyer

Department of ECE, NIIT University, Neemrana, Alwar, Rajasthan, India

Abstract: This paper formulates a framework for solving the offline physical layer impairment-routing and wavelength assignment (PLI-RWA) issue in translucent wavelength division multiplexed (WDM) optical networks. For network design, the PLI-Signal Quality Aware RWA (PLI-SQARWA) algorithm is employed that (a) guarantees zero blocking due to signal degradation and wavelength contention and (b) minimizes the total required number of regenerators and all-optical wavelength converters (AOWCs). Further, in view of a latency efficient technology capable of delivering a cost effective implementation suitable for large scale deployment, our previously proposed novel electro-optical hybrid translucent nodes are deployed within the network. Unlike our previous studies which assumed the use of full range wavelength converter (FRWC) within the hybrid node, in the current study, from a practical perspective, we use limited range wavelength converter (LRWC) in order to resolve wavelength conflicts. For network equipped with the hybrid nodes and employing PLI-SQARWA, performance results are presented, in presence of FRWCs and LRWCs respectively.

Keywords: Translucent wavelength division multiplexed (WDM) network, regenerator placement, wavelength converter placement, FRWCs, LRWCs, PLI-SQARWA.

1. Introduction

In today's optical backbone networks typically employing wavelength-division multiplexing (WDM), the traffic flow is increasing steadily and becoming more heterogeneous. Different types of new applications such as, IPTV, VoD, VoIP, etc., require high bit-rate transmission and are associated with different bandwidth granularities of traffic demands that converge on the optical backbone network. However, with increase in the bit-rate, the investment on regenerator cards increases, since the high-bit-rate paths have limited transmission reach, and the physical layer impairments (PLIs) start to significantly limit reach of the regenerator-free optical distance [1, 2]. In view of the accumulation of PLIs, in recent years, a cross layer design methodology has been adopted for WDM network design which has stirred a new trend by accounting for the impact of PLIs on optical reach of the signal(s) in the so called PLI-routing and wavelength assignment (PLI-RWA) techniques [3]. Further, the establishment of non-feasibility of both, opaque and transparent networks has led to the emergence of sparse regeneration based translucent networks, for which, the PLI-RWA approaches mainly focus on (a) the regenerator placement (RP) problem and/or (b) the regenerator allocation (RA) problem [3]. According to the current state of art, introduction of regenerators for provisioning demands due to signal quality and/or wavelength contention requirements inevitably disrupts transparency of the signal(s) and simultaneously introduces unnecessary delay, since regenerators involve the optical-electrical-optical (OEO) conversion process which incurs more time than switching in the optical domain. Further, acknowledging that an optical port is five times less expensive than an electrical one [4], regenerators also substantially increase the overall network cost. The aforementioned inadequacies of regenerator introduction within the network act as significant performance bottlenecks which has led to minimizing the total number of network regenerators as one of the major objectives in translucent WDM network design [3].

In view of the above, the authors in [5] proposed to solve the translucent network design problem by introducing a heuristic called Cross-Optimization for RWA and RP (COR2P) which aims at minimizing both, the number of required regenerators and number of regeneration sites. The authors have shown that COR2P (a) results in regenerator concentration in few network nodes (sites), (b) does not reject any demands for low or moderate traffic, and (c) reduces the total number of regenerators. In our previous works [6, 7 and 8], we have proposed two novel algorithms that overcome the deficiencies of COR2P. In [6, 7], the introduced PLI-Signal Quality Aware RWA (PLI-SQARWA) algorithm (a) employs the signal quality aware routing (SQAR) that finds candidate routes which use fewest amounts of

regenerators, and (b) maximally uses placed regenerators for wavelength conversion (WC), before resorting to all-optical wavelength converters (AOWCs); thus, being able to minimize the total network components. The results show that PLI-SQARWA guarantees zero signal and wavelength blocking and outperforms COR2P in terms of network components, while demonstrating similar blocking performance to COR2P at various traffic loads. In [8], we introduced the innovative PLI-signal quality and delay aware RWA (PLI-SQDARWA) algorithm that is founded on signal quality and delay aware routing (SQDAR) approach, which evaluates candidate routes considering both, signal quality and end-to-end delay. We have shown through extensive simulations that for all traffic load values, PLI-SQDARWA guarantees low blocking and outperforms COR2P in terms of latency. Further, a delay analysis for the network based on PLI-SQDARWA shows that for any network configuration, there exists a trade-off between delay incurred for obtaining and maintaining the desired QoT.

In all of our previous works [6, 7 and 8], the AOWCs used for wavelength contention resolutions were assumed to be ideal or full range wavelength converters (FRWCs). However, such an assumption may not be valid in practical networks since, no wavelength converter has full-range wavelength translation capability [9]. Hence, an important challenge in network design is to overcome the limitations while using limited range wavelength converters (LRWCs). The authors in [9] have shown that the performance of such converters based on four wave mixing (FWM) in semiconductor optical amplifier (SOA) is a strong function of the difference between the wavelength converter's input and output frequencies i.e., for a particular input frequency (wavelength), conversion to some output frequencies results in an output signal which is significantly degraded; hence leading to limitations in the conversions which can be performed.

In this paper, we extend our previous studies by designing a framework that corroborates the offline version of PLI-RWA problem in translucent networks where, given a network topology and estimate of traffic demands, the static PLI-RWA, wavelength converter placement (WCP) and RP problems are solved jointly. The novelty of the current work is twofold:

- The previously proposed innovative PLI-SQARWA algorithm [6, 7] is implemented for network design considering the deployment of LRWCs within the network. We then proceed to the performance comparison of PLI-SQARWA based on the use of FRWCs and LRWCs respectively.

- The network model consists of the deployment of our previously proposed electro-optical hybrid translucent nodes [10], which is a latency efficient technology capable of delivering a cost effective implementation suitable for large scale deployment.

This paper is organized as follows. Section 2, describes the network model and analyzes the network performance in presence of FRWCs and LRWCs, respectively. In section 3, we present the numerical results wherein, we detail performance evaluation results of the network employing the PLI-SQARWA algorithm and comprising of FRWCs and LRWCs respectively. Finally, Section 4 presents the conclusion of this study.

2. Network Model

The WDM translucent network architecture shown in Fig. 1 assumes that each input is connected to each output on every wavelength. In order to interconnect a set of users connected to different star couplers and using wavelength routers, the path is established through optical cross connects (OXCs), which comprise of the hybrid translucent nodes [10]. A lightpath transiting such a node is switched transparently (L_1) or directed to the regenerator pool (L_2) if 1) it requires only regeneration or, 2) it simultaneously requires both regeneration and WC. If only wavelength contention is to be resolved, the lightpath is directed to the wavelength converter (L_3), which is based on the FWM in SOA model [9].

The network is based on an Intensity Modulation/Direct Detection (IM/DD) system employing on-off keying (OOK) non-return-to-zero (NRZ) modulation, with N equally spaced channels having equal power. The lightpath quality of transmission (QoT) evaluation is based on the realistic estimation of signal quality considering the simultaneous impact of stimulated Raman scattering (SRS), FWM, wavelength converter and amplified spontaneous emission (ASE) noise. In view of longer optical reach of the signals, with the aim of minimizing the OEO regenerators, and hence reducing the overall network cost, in the current study, we have considered channels operating at a bit-rate of 10 Gb/s; hence, the FWM effect is the dominant PLI [11]. We assume fiber links to be deployed using standard single mode non-zero dispersion shifted fibers, and erbium doped fiber amplifiers (EDFAs) to be deployed every fiber span (typically every 80Km) in order to recover from fiber losses.

In the network shown in Fig. 1, the star couplers distribute the input power equally among all N output ports and the amplifiers are considered to have a uniform gain G over the optical bandwidth B_0. Each receiver receives the signal on all wavelengths and optical filters are used to filter out the required wavelength. The received signal is then detected with the help of a photo detector. Let P_t denote the transmitted power and assuming that data bits '1' and '0' are transmitted as a "mark" and "space" respectively, the signal power for bit '0' is assumed to be zero.
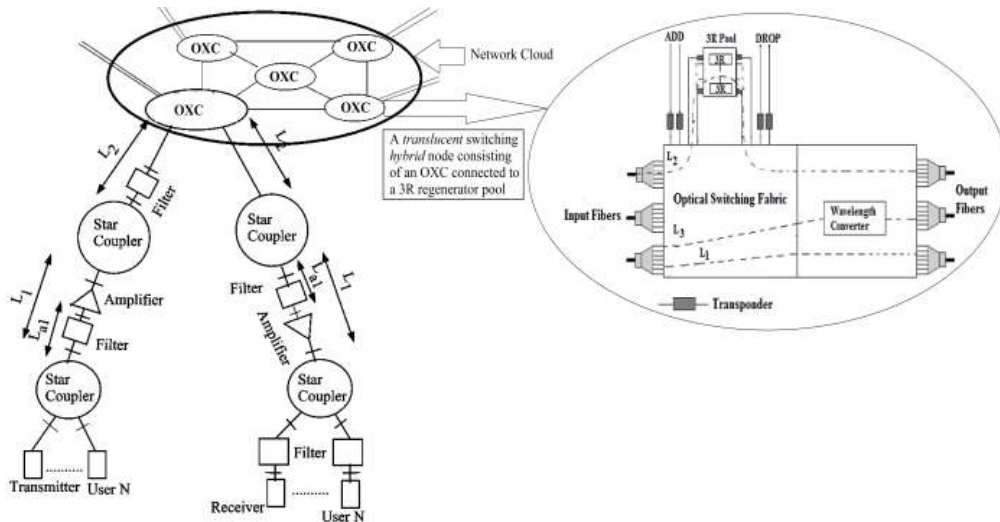
Figure 1: Architecture of the WDM translucent network

2.1.   Network Performance Evaluation in presence of FRWC

In this sub-section, we analyze the network performance when the AOWCs within the hybrid nodes of the OXCs are FRWCs. Since FWM is the dominant PLI, maximum number of FWM components will be generated at the central channel [11]. Hence, the worst affected channel is the central channel, which is represented as the jth channel. The effect of SRS at the jth channel will lead to power reception from channels 1 to j-1 and power transfer to channels j+1 to N. The depleted and the gained powers, represented as P_- and P_+, are given as [11]

$$P_-(dB) = \sum_{i=j+1}^{N} \left(\frac{\lambda_i}{\lambda_j}\right) \frac{(i-1)P\Delta f g_p L_{eff} 10 \log_{10} e}{3 \times 10^{13} A_{eff}} m_i \tag{1}$$

and

$$P_+(dB) = \sum_{i=1}^{j-1} \frac{(i-1)P\Delta f g_p L_{eff} 10 \log_{10} e}{3 \times 10^{13} A_{eff}} m_i \tag{2}$$

respectively. Hence, the signal power $P_{SRS(s,j)}^{(r)}$ at the jth receiver will be

$$P_{SRS(s,j)}^{(r)}(dBm) = P_t(dBm) - P_-(dBm) + P_+(dBm) + 2G(dB) - \alpha\left[2(L_1 + L_2)\right]$$
$$- 11L_{sp} - 4L_{cv} - 2L_{ti} - 2L_{ti}^* + 20\log N + 20\log N_{star} \tag{3}$$

where α is the fiber loss coefficient in dB/km, L_{sp} the splicing loss (at splices marked as "/" in Fig. 1), L_{cv} the loss due to non-uniformity in power splitting by the star coupler, L_{ti} the total insertion loss of the star coupler and N_{star} the number of output ports of the star coupler that uses passive wavelength routers. The distance between the broadcast star that uses optical terminals and the amplifier is L_{a1}. Further, distance between the broadcast star that uses optical terminals and the star coupler interconnecting such a set is L_1, while, distance between the OXC and the star coupler that uses passive wavelength routers is L_2. It must be noted that (a) when the AOWC within the hybrid node is assumed to be a FRWC, wavelength converter noise due to the AOWC will not be incurred, and (b) when a regenerator is used to resolve wavelength conflict(s), it acts as a FRWC and hence, the analysis presented in this section is used for network performance evaluation. The total electric field at the receiver is given by

$$E(t) = B_s \sqrt{2P_{SRS(s,j)}^{(r)}} \cos(\omega_j t) + \sqrt{2P_{FWM}^{(r)}} \cos(\omega_j t - \theta_{FWM}) +$$
$$\sum_{k=-M}^{M} \sqrt{2P_{sp}\delta v} \cos((\omega_j t + 2\pi k\delta v) + \varphi_k) \tag{4}$$

where first term is the electric field due to signal component while, the second and third terms represent the electrical fields due to FWM and ASE noise respectively. In (4), φ_k is a random phase for each component of spontaneous emission, $P_{sp} = S_{sp} \cdot B_0$ and $M = \frac{B_0}{2\delta v}$. The receiver current for bit '1', $i_1(t)$ (i.e. B_s=1) is given by

$$i_1(t) = R_0 \overline{E^2(t)} \tag{5}$$

where

$$R_0 \overline{E^2(t)} = R_0 P_{SRS(s,j)}^{(r)}[1 + \cos(2\omega_j t)] +$$
$$2R_0 S_{sp}\delta\nu \left[\sum_{k=-M}^{M} \cos((\omega_j t + 2\pi k\delta\nu) + \phi_k) \right]^2 +$$
$$4R_0 \sum_{k=-M}^{M} \left(\begin{array}{c} \sqrt{P_{SRS(s,j)}^{(r)} S_{sp}\delta\nu} \cos(\omega_j t) \cdot \\ \cos((\omega_j t + 2\pi k\delta\nu) + \phi_k) \end{array} \right) +$$
$$4R_0 \sqrt{\left(\begin{array}{c} P_{FWM}^{(r)}(1) \cdot \\ S_{sp}\delta\nu \end{array} \right)} \sum_{k=-M}^{M} \left(\begin{array}{c} \cos(\omega_j t - \theta_{FWM}) \cdot \\ \cos((\omega_j t + 2\pi k\delta\nu) + \phi_k) \end{array} \right) +$$
$$4R_0 \sqrt{P_{SRS(s,j)}^{(r)} P_{FWM}^{(r)}(1)} \cos(\omega_j t)\cos(\omega_j t - \theta_{FWM})$$

(6)

In the above equation, S_{sp} represents the power spectral density of ASE noise at the receiver which is given as

$$S_{sp} = \left[\frac{S_{sp,out}G}{L^*} + \frac{n_{sp}(G-1)hf_s}{L^{**}} \right]$$

(7)

where $L^{**} = \alpha[(L_1 - L_{a1})] + 3L_{sp} + L_{cv} + L_{ti} + 10\log N$, and $L^* = \alpha[(L_1 + L_2)] + 5L_{sp} + 2L_{cv} + L_{ti} + L_{ti}^* + 10\log N + 10\log N_{star}$.

In (7), n_{sp} is the spontaneous emission factor and $S_{sp,out}$ the ASE noise power spectral density at the output of the OXC which is given as

$$S_{sp,out} = S_{sp,in}G + (G+1)n_{sp}hf_s$$

(8)

where $S_{sp,in}$ represents the power spectral density of ASE noise at input of the OXC and is given as

$$S_{sp,in} = \frac{n_{sp}(G-1)h\nu}{L^{***}}$$

(9)

where $L^{***} = \alpha[(L_2 + L_1 - L_{a1})] + 3L_{sp} + L_{cv} + L_{ti}^*$.

In (6), first term represents the signal. The second term gives rise to ASE-shot beat noise and ASE-ASE beat noise, third term ASE-signal beat noise, fourth term FWM-ASE beat noise and fifth term FWM-signal beat noise respectively. The third, fourth and fifth terms have zero mean. The receiver current for bit '1' will be the sum of currents due to individual components and thermal noise. Thus, the mean value of current for bit '1' is given by

$$\langle i(1) \rangle = R_0 P_{SRS(s,j)}^{(r)} + R_0 S_{sp} B_0$$

(10)

The noise variance for bit '1' is

$$\sigma^2(1) = 2eR_0 P_{SRS(s,j)}^{(r)} B_e + 2eR_0 S_{sp} B_e B_0 +$$
$$4R_0^2 P_{SRS(s,j)}^{(r)} S_{sp} B_e + R_0^2 S_{sp}^2 [2B_e B_0 - B_e^2] +$$
$$R_0^2 P_{SRS(s,j)}^{(r)} \langle P_{FWM}^{(r)}(1) \rangle + 2R_0^2 \langle P_{FWM}^{(r)}(1) \rangle S_{sp} B_e +$$
$$4K_B T B_e / R_L$$

(11)

where R_0 is the responsivity, e the electron charge, K_B the Boltzmann constant, B_e the electrical bandwidth of the receiver, T the receiver temperature and R_L the load resistance. In (11), the value of $\langle P_{FWM}^{(r)}(1) \rangle$ is given as [11]

$$\langle P_{FWM}^{(r)}(1) \rangle = 2\left[\frac{1}{8} \sum_{k \neq l \neq m} P_{klm}^{(r)} + \frac{1}{4} \sum_{k \neq l \neq m=1} P_{kl1}^{(r)} + \frac{1}{4} \sum_{k=l \neq m} P_{kkm}^{(r)} \right]$$

(12)

The expression for $R_0 E^2(t)$ when bit '0' (i.e., $B_s = 0$ and $P_s^{(r)} = 0$) is transmitted is

$$R_0 E^2(t) = P_{FWM}^{(r)}(0)R_0 +$$
$$2R_0 S_{sp}\delta\nu \left[\sum_{k=-M}^{M} \cos((\omega_j t + 2\pi k\delta\nu) + \varphi_k) \right]^2$$
$$+4R_0 \sqrt{P_{FWM}^{(r)}(0)S_{sp}\delta\nu} \cdot$$
$$\left[\sum_{k=-M}^{M} \cos(\omega_j t - \theta_{FWM})\cos((\omega_j t + 2\pi k\delta\nu) + \varphi_k) \right]$$

(13)

Hence, the mean value of current $i_0(t)$ represented as $\langle i(0) \rangle$ is given by

$$\langle i(0) \rangle = R_0 \langle P_{FWM}^{(r)}(0) \rangle + R_0 S_{sp} B_0 \tag{14}$$

where $\langle P_{FWM}^{(r)}(0) \rangle$ is given as [11]

$$\langle P_{FWM}^{(r)}(0) \rangle = 2 \left[\frac{1}{8} \sum_{k \neq l \neq m} P_{klm}^{(r)} + \frac{1}{4} \sum_{k=l \neq m} P_{kkm}^{(r)} \right] \tag{15}$$

The noise variance for bit '0' is

$$\sigma^2(0) = 2eR_0 S_{sp} B_0 B_e + R_0^2 S_{sp}^2 [2B_e B_0 - B_e^2] +$$
$$\sigma_{FWM-ASE}^2(0) + 4K_B T B_e / R_L \tag{16}$$

where [9]

$$\sigma_{FWM-ASE}^2(0) = 4R_0^2 \langle P_{FWM}^{(r)}(0) \rangle \cdot S_{sp} B_e \tag{17}$$

The probability of bit error, which specifies the average probability of incorrect bit identification, is given as [12]

$$BER = \frac{1}{2} \left(\frac{Q}{\sqrt{2}} \right) \tag{18}$$

The Q-factor related to signal to noise ratio in order to achieve a specific probability of bit error is given as [13]

$$Q = \frac{\langle i(1) \rangle - \langle i(0) \rangle}{[\sigma(1) - \sigma(0)]} \tag{19}$$

where $\langle i(1) \rangle$ and $\langle i(0) \rangle$ represent the mean values of current $i_1(t)$ and $i_0(t)$, and $\sigma(1)$ and $\sigma(0)$ represent the variance values for bit '1' and bit '0' respectively. Substituting $\langle i(1) \rangle$, $\langle i(0) \rangle$ from (10) and (14) into (19), we obtain

$$Q = \frac{R_0 P_{SRS(s,j)}^{(r)} - \left(2R_0 P_{SRS(s,j)}^{(r)} \cdot \left[\frac{1}{8} \sum_{k \neq l \neq m} \frac{P_{klm}^{(r)}}{P_{SRS(s,j)}^{(r)}} + \frac{1}{4} \sum_{k=l \neq m} \frac{P_{kkm}^{(r)}}{P_{SRS(s,j)}^{(r)}} \right] \right)}{\sigma(1) + \sigma(0)} \tag{20}$$

Once $\sigma(1)$ and $\sigma(0)$ are known, $P_{SRS(s,j)}^{(r)}$ can be determined for a given Q (or P_e) from (20). With this value of $P_{SRS(s,j)}^{(r)}$, corresponding P_t can be determined from (3). The above Q-factor model is used to evaluate blocking probability (BP) which is the performance metric used in our study. BP is defined as the probability that a connection cannot be accepted and is given as

$$Blocking\ Probability = \frac{Number\ of\ blocked\ connections}{Total\ number\ of\ offered\ connections} \tag{21}$$

When the receiver Q-factor associated with a connection request is below the threshold, the connection is blocked.

2.2. Network Performance Evaluation in presence of LRWC

In this sub-section, we analyze the network performance when the AOWC within the hybrid node of the OXC is a LRWC. We use the LRWC model based on FWM in SOA wherein; the LRWC is characterized by the conversion efficiency (η_{wc}) and the ASE power spectral density (S_{sp}) [9]. In such a model, translations of k wavelengths are allowed either side of the input wavelength and hence, the allowed output wavelengths are limited to a certain symmetrical range either side of the input wavelength. Therefore, the LRWC can translate up or down from a given input wavelength, which is defined by the translation degree. Thus, 100% translation degree implies full-range wavelength translation whereas, 0% translation degree implies no translation. In this case, the signal power $P_{SRS(s,j)}^{(r)*}$ at the jth receiver will be given as:

$$P_{SRS(s,j)}^{(r)*} = P_t(dBm) - P_-(dBm) + P_+(dBm) + 2G(dB) - \eta_{wc} - \alpha[2(L_1 + L_2)] - 11L_{sp} - 4L_{cv} - 2L_{ti} - 2L_{ti}^* + 20\log N + 20\log N_{star} \tag{22}$$

where η_{wc} represents the conversion efficiency of the wavelength converter. The total electric field at the receiver is given by

$$E(t) = B_s \sqrt{2P_{SRS(s,j)}^{(r)*}} \cos(\omega_j t) + \sqrt{2P_{FWM}^{(r)*}} \cos(\omega_j t - \theta_{FWM}) + \sum_{k=-M}^{M} \sqrt{2P_{sp}^* \delta v} \cos((\omega_j t + 2\pi k \delta v) + \varphi_k) \tag{23}$$

where first term is the electric field due to signal component while, the second and third terms represent the electrical fields due to FWM and ASE noise respectively. In (23), $P_{sp}^* = S_{sp}^* \cdot B_0$, where the power spectral density of ASE noise at the receiver, denoted as S_{sp}^*, is given as

$$S_{sp}^* = \left[\frac{S_{sp,out}^* G}{L^*} + \frac{n_{sp}(G-1)h f_s}{L^{**}} \right] \tag{24}$$

where, due to the presence of LRWC, the ASE noise power spectral density at the output of the OXC, denoted as $S_{sp,out}^*$, will be given as

$$S_{sp,out}^* = \left[\frac{S_{sp,in}^* G}{\eta_{wc}} \right] + G\left[\frac{n_{sp}h f_s}{\eta_{wc}} \right] + \left[n_{sp}h f_s \right] \tag{25}$$

where power spectral density of ASE noise at the input of OXC, denoted as $S_{sp,in}^*$, will be equal to $S_{sp,in}$, and is as given in (9). The FWM power at input of the OXC is given as

$$P_{FWM,in}^* = \left[\frac{P_{klm} G}{L_{FWM}} \right] \tag{26}$$

where $L_{FWM} = \alpha(L_2 + L_1 - L_{a1}) + 4L_{sp} + \alpha(L_2) + L_{cv} + L_{ti}^* + 10 \log N_{star}$ represents the loss in FWM signal from the point of generation to the OXC. The FWM power at output of the OXC is given as

$$P_{FWM,out}^* = \left[\frac{P_{FWM,in}^*}{\eta_{wc}} \right] \tag{27}$$

The FWM power at the receiver in terms of FWM power at the output of the OXC is given as

$$P_{FWM}^{(r)*} = \left[\frac{P_{FWM,out}^* G}{L_{FWM}^*} \right] \tag{28}$$

where $L_{FWM}^* = \alpha(L_2 + L_1) + 5L_{sp} + 2L_{cv} + L_{ti} + L_{ti}^* + 10 \log N + 10 \log N_{star}$.

Using (26), (27), and (28) FWM power at the receiver can be obtained, and hence, the ratio of FWM power to signal power at the receiver can be evaluated as

$$\frac{P_{klm}^{(r)}}{P_{SRS(s,j)}^{(r)*}} = d^2 k^* \left[\frac{1 - \exp[-\alpha_N L_{a1}]^2 + 4\exp[-\alpha_N L_{a1}]\sin^2(\Delta\beta L_{a1}/2)}{\alpha_N^2 + \Delta\beta^2} \right] \tag{29}$$

where α_N is an equivalent representation for fiber loss coefficient in neper/km, $\Delta\beta$ the phase mismatch, d the degeneracy factor and P_0 the input power to the fiber. In (29), the parameter k^* is given as

$$k^* = \frac{1024\pi^6}{n^4 \lambda^2 c^2} \left[\frac{\chi_{111}}{A_{eff}} \right]^2 \tag{30}$$

where λ is the optical wavelength, c the speed of light in vacuum, A_{eff} the effective cross-sectional area of fiber core in square meter, n the refractive index and χ_{111} the third-order non-linear susceptibility.

As the ASE noise power spectral density, signal power, and the ratio of FWM power to signal power at the receiver are known, noise variances for bits "1" and "0" (i.e., σ (1) and σ (0)) can be evaluated using (11) and (16). Finally, the Q-factor value in this case will be evaluated as

$$Q = \frac{R_0 P_{SRS(s,j)}^{(r)*} - \left(2R_0 P_{SRS(s,j)}^{(r)*} \cdot \left[\frac{1}{8} \sum_{k \neq l \neq m} \frac{P_{klm}^{(r)}}{P_{SRS(s,j)}^{(r)*}} + \frac{1}{4} \sum_{k=l \neq m} \frac{P_{kkm}^{(r)}}{P_{SRS(s,j)}^{(r)*}} \right] \right)}{\sigma(1) + \sigma(0)} \tag{31}$$

As σ (1) and σ (0) are known, $P_{SRS(s,j)}^{(r)*}$ can be determined for a given Q (or P_e) from (31). With this value of $P_{SRS(s,j)}^{(r)*}$, corresponding P_t can be determined from (22). Once, the Q-factor value is known, the BP can be determined using (21).

3.   Numerical Results

Following the analysis in section 2 for the network shown in Fig. 1, we performed a similar analysis in order to investigate the 18 node NSFNET network depicted in Fig. 2, which is based on 50 GHz channel spacing. The PLI-SQARWA algorithm [6, 7] selects the appropriate deployment of regenerator(s) and/or wavelength converter(s) within the hybrid translucent node(s). For analysis, Q-factor threshold takes the value of 6 which corresponds to a BER of 10^{-9}. We consider permanent lightpath demands (PLDs) which are offline requests that consist of pre-known connection demands with data rate equal to full capacity of the wavelength channel and are thus established through a full lightpath.
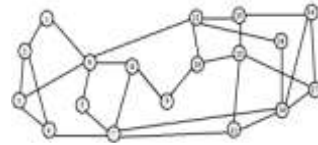

Figure 2: 18 node NSFNET network.

The simulations cover six traffic loads that range from 100 to 600 connection demands and for each load, 10 static traffic matrices are generated stochastically according to uniform distribution. Thus, presented results are average values of ten simulation runs. Table 1 summarizes the various transmission system parameters adopted in our simulations. Further, in order to appropriate the investigation of number of non-accepted requests by PLI-SQARWA, in the current study, for all traffic load values and comparison based on the deployment of FRWCs and LRWCs, we chose simulation parameters such that cases admitting a solution did not guarantee 0% of resource blocking.

Table 1: Transmission System Parameters.

Parameters	Values
Wavelength spacing (Δf) (GHz)	50
SMF losses (dB/km)	0.2
Raman gain profile (cm/W^2) [11]	7×10^{-12}
Quantum efficiency of photo detector (n)	0.95
Output power variability of NxN coupler (L$_{cv}$) (dB)	0.5
Laser power/channel (dBm/channel)	3
SMF dispersion (ps/nm.km)	17
Insertion loss of each 2x2 Coupler (L$_{ti}$) (dB)	0.5
Splice loss (L$_{sp}$) (dB)	0.5
Bit Rate (Gbps)	10
Core area of the fiber (A$_{eff}$) (μm^2)	50
Load Resistance (R$_L$)	100
Receiver temperature (T)	300
ASE Factor (n_{sp}) [9]	1.5
Number of wavelengths	16 and 32
Nonlinear refractive index of fiber (n$_2$) (m^2/W) [11, 12]	2.7×10^{-20}
Optical filter bandwidth (GHz)	10
Unsaturated amplifier gain (G) (dB)	10
Electrical bandwidth of receiver (GHz)	1
Input EDFA gain (dB)	22
Output EDFA gain (dB)	16
Switch crosstalk ratio (dB) [10]	32
Converter efficiency (η_{wc}) (dB) [9]	-6.5
ASE power spectral density (S_{sp}) (W/Hz) [9]	1.63×10^{-8}

In Fig. 3, variation of BP with traffic load for different degrees of translation of the wavelength converter has been plotted for the PLI-SQARWA algorithm when the network provisions 16 wavelengths per fiber link. It can be observed from the figure that

i.   Both, regeneration and WC is provisioned which eradicates blocking due to signal degradation and wavelength contention respectively, and

ii.   Owing to low loads, the network is not overloaded and ample resources are available.

1.   For intermediate and high traffic loads (beyond 300 demands) with 100% translation, negligible resource blocking starts to occur for PLI-SQARWA due to the selection of few shortest paths as candidate routes. Overall, the demonstrated BP is low since for PLI-SQARWA, rather than the shortest paths, majority of the 'Best Paths' are selected as the candidate routes, which leads to larger resources being available even at higher traffic loads.

2.   A significant proportion of the performance improvement introduced by FRWCs is obtained with increase in the translation degree of LRWCs. At a traffic load of 400 PLDs, the BP for 40% of full range conversion is 7.49×10^{-5}, which decreases to 4.01×10^{-5} for 60% of full range conversion, and which further reduces to 2×10^{-5} when 80% of full range translation is present. It can also be observed that when 100% translation is provisioned, a value of 2×10^{-5} is obtained, which is similar to the value obtained when 80% of full range translation is provisioned. A similar trend is observed when the traffic load increases. Hence, it can be inferred that almost all of the improvement introduced by full-range translation is obtained with limited-range translation by approximately half the full range.
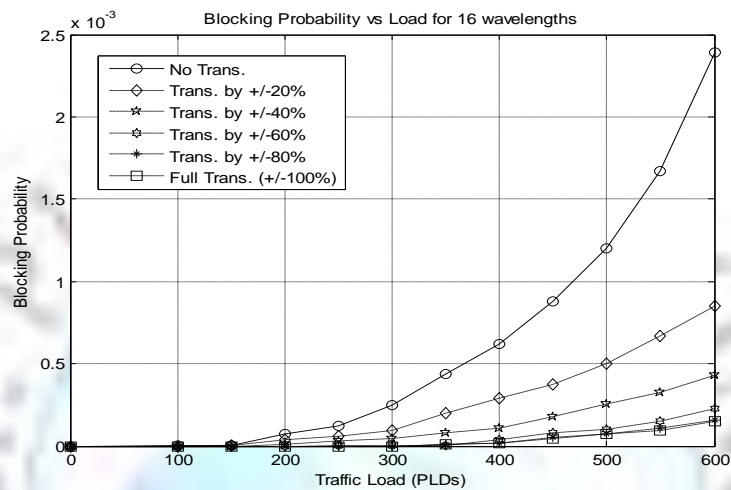

Figure 3: Blocking Probability versus traffic load for PLI-SQARWA with FRWCs and LRWCs.

It can also be inferred from Fig. 3 that for low loads with 100% translation, PLI-SQARWA accepts all the demands whereas, between moderate and high loads, it is able to maintain acceptable blocking. However, the deployment of LRWCs results in blocking even at low loads owing to the presence of wavelength converter noise. Further, higher values of translation degree for a LRWC provisions more available wavelengths for lightpath establishment. Hence, higher translation range LRWCs only decrease the wavelength-related blocking whereas, regenerators only reduce the BER (Q-factor)-related blocking. Thus, both, AOWCs and regenerators are requisited in order to reduce the overall network blocking.

Fig. 4 and 5 show the variation of Q-factor with the transmitted power, when number of wavelengths provisioned by the network are 16 and 32, respectively.
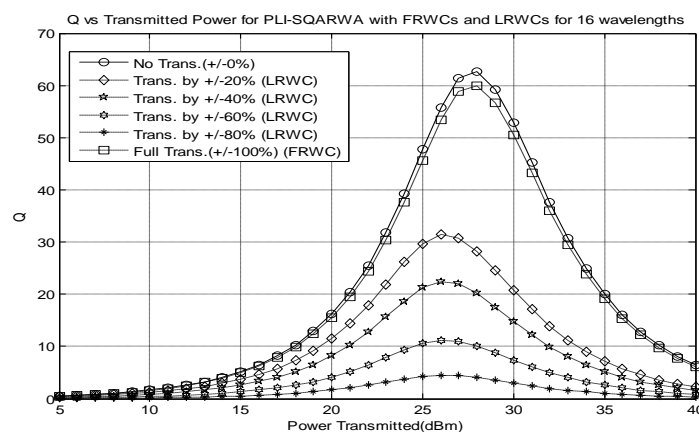

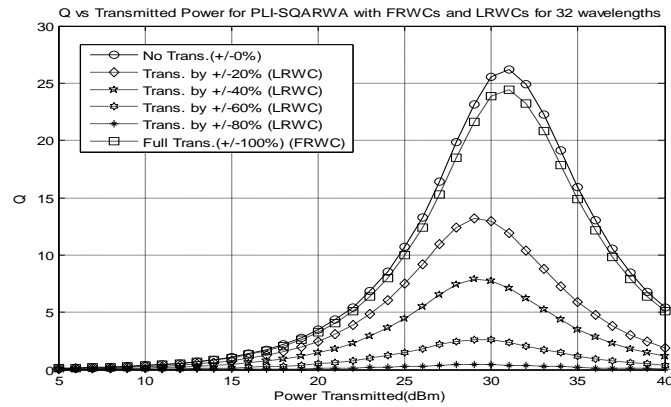Figure 4: Variation of Q-factor with transmitted power for 16 wavelengths.

Figure 5: Variation of Q-factor with transmitted power for 32 wavelengths.

It can be observed from the figures that

1. When wavelength translation is not allowed (i.e. 0% translation) and the network provisions 16 wavelengths (Fig. 4), at low transmitted power, the value of Q increases with increase in the transmitted power. However, as the transmitted power is increased, after a certain power level, the FWM power becomes dominant and Q-factor performance of the network starts degrading. A similar variation of Q with transmitted power is observed when the number of wavelengths provisioned by the network is increased to 32 (Fig. 5). However, with increase in number of wavelengths (a) the transmitted power required to obtain a given Q increases, and (b) the maximum value of Q that can be achieved decreases, since both, the number of generated FWM components and the power loss in the splitter increase with an increase in the number of wavelengths. The maximum value of Q achievable when the network provisions 16 wavelengths is 62.59 (Fig. 4), which decreases to 26.16, when number of wavelengths provisioned by the network is increased to 32 (Fig. 5). This is due to combined effect of thermal, shot, SRS, FWM and ASE noises.

2. When wavelength translation is provisioned, a similar trend of Q with transmitted power is observed as is seen when wavelength translation is not provisioned. However, for a given transmitted power, compared to when wavelength translation is not provisioned, (a) use of FRWCs gives approximately the same Q values as when no translation is provisioned, since both, 0% translation and ideal WC do not introduce any wavelength converter noise and hence, do not alter the Q values, and (b) Q values degrade with the introduction of LRWCs, owing to the presence of wavelength converter noise.

3. When wavelength translation is provisioned, for a given transmitted power, compared to when the translation degree value is lower, Q values degrade for higher translation degrees of the wavelength converter, which can be attributed to the presence of higher wavelength converter noise. It can be observed from Fig. 4 that, when the number of wavelengths provisioned by the network is 16, the maximum value of Q is 22.48, when wavelength converter with 40% translation degree is used. The Q value decreases to 11.24, with the use of a wavelength converter with 60% translation degree; and further to 4.49, with the use of a wavelength converter with 80% translation degree, respectively. This occurs since the difference between input and output wavelengths of the wavelength converter affects the network performance wherein; larger difference between the input and output wavelengths degrades the performance. For e.g., in case of network provisioning 16 wavelengths, with the values of k as 6 (i.e. 40% translation degree), and 12 (i.e. 80% translation degree) respectively, network performance when conversion is from $\lambda_1 \rightarrow \lambda_6$ is better than when the conversion is from $\lambda_1 \rightarrow \lambda_{12}$. A similar trend is observed when the number of wavelengths provisioned by the network is increased to 32 (Fig. 5). It is also observed in this case that the use of FRWCs provides approximately the same Q-factor performance as when no wavelength conversion is provisioned.

4. Conclusion

In this paper, we employed the PLI-SQARWA algorithm and deployed the novel electro-optical hybrid translucent nodes for network design. In addition, opposed to the assumption of use of FRWCs within the hybrid nodes as in our previous studies, in the current study, we deployed the more practical LRWCs within the hybrid nodes for wavelength contention resolutions. The network performance results clearly show that in the presence of FRWCs, PLI-SQARWA is able to accept all the demands at low traffic loads, and presents negligible blocking at moderate and high loads. However, the introduction of LRWCs within the network results in higher blocking owing to the presence of wavelength converter noise. Further, higher translation range LRWCs only decreases the wavelength-related blocking whereas; regenerators only reduce the BER-related blocking. Thus, both, AOWCs and regenerators are requisited in order to reduce the overall

network BP. The results also indicate that (a) significant improvement in blocking performance of the network is obtained when LRWCs with as little as 20% of the full range are introduced, (b) almost all of the network performance improvements offered by FRWCs is obtained from LRWCs with approximately half of the full translation range, and (c) in the presence of LRWCs, network performance depends on difference between the input and output wavelengths. Further, it is observed that (a) for large numbers of wavelengths, low values of translation degree and large difference between the input and output wavelengths of the wavelength converter, it is not be possible to obtain the desired Q-factor performance, and (b) the use of FRWCs gives approximately the same Q-factor values as when 0% translation is provisioned, since in both the cases, no wavelength converter noise is introduced and hence, Q-factor values are not altered. In conclusion, it is an important issue as to how to choose the optimal number of wavelengths and translation degree of a wavelength converter such that the desired performance can be achieved.

References

[1]. J. Berthold, A. Saleh, L. Blair and J. Simmons, "Optical networking: Past, present, and future," IEEE/OSA Journal of Lightwave Technology, vol. 26, no. 9, pp. 1104–1118, 2008.

[2]. J.M. Simmons, "On determining the optimal optical reach for a long-haul network", IEEE/OSA Journal of Lightwave Technology, vol. 23, no. 3, pp. 1039–1048, 2005.

[3]. S.P. Singh, S. Iyer, S. Kar and V. K. Jain, "Study on Mitigation of Transmission Impairments and Issues and Challenges with PLIA-RWA in Optical WDM Networks", Journal of Optical Communication, De Gruyter, vol. 33, no. 2, pp. 83-101, 2012.

[4]. M. Gagnaire and S. Al Zahr, "Impairment-Aware Routing and Wavelength Assignment in Translucent Networks: State of the Art", IEEE Communications Magazine, vol. 47, no. 5, pp. 55-61, 2009.

[5]. M. Youssef, S. Al Zahr and M. Gagnaire, "Translucent network design from a CapEx/OpEx perspective", Photonics Network Communications, vol. 22, no. 1, pp. 85–97, 2001.

[6]. S. Iyer and S.P. Singh, "A Novel Offline PLI-RWA and Hybrid Node Architecture for Zero Blocking and Time Delay Reduction in Translucent Optical WDM Networks", Communications and Networks, Scientific Research, vol. 4, no. 4, pp. 306-321, 2012.

[7]. S. Iyer and S.P. Singh, A Novel offline PLI-RWA, Regenerator Placement and Wavelength Converter Placement Algorithm for Translucent Optical WDM Networks", in Proc. IEEE Signal Processing and Communications (SPCOM), pp. 1-5, 2012.

[8]. S. Iyer and S.P. Singh, "A Novel Signal and Delay Aware, Zero Blocking PLI-RWA and Translucent Node Architecture for Optical WDM Networks", International Journal of Computer and Electrical Engineering (IJCEE), vol. 5, no. 5, pp. 492-499, 2013.

[9]. S.P. Singh, S. Kar, S and V.K. Jain, "Performance of All-Optical WDM Network in Presence of Four-Wave Mixing, Optical Amplifier Noise, and Wavelength Converter Noise", Fiber and Integrated Optics, vol. 26, no. 2, pp. 79-97, 2007.

[10]. S. Iyer and S.P. Singh, "A Novel Hybrid Node Architecture for Reducing Time Delay in Wavelength Division Multiplexed (WDM) Translucent Network", in Proc. IEEE National Conference on Communications (NCC), pp. 1-5, 2012.

[11]. S. Iyer, and S.P. Singh, "Impact of combined nonlinearities and ASE noise on Performance of 10 Gbps all Optical Star WDM Networks", Communications and Networks, Scientific Research, vol. 3, no. 4, pp. 235-249, 2011.

[12]. S. Iyer and S.P. Singh, "Theoretical Evaluation of combined nonlinearities and ASE noise Penalties in Optical Star WDM Networks Based on ITU-T conforming Optical Fibers", The Institution of Electronics and Telecommunication Engineers (IETE) Journal of Research, vol. 58, no. 6, pp. 482-492, 2012.

[13]. G.P. Agrawal, "Fiber Optic Communications Systems", Wiley & Sons, New York, 2002.